A Comprehensive Electrical-Gas-Hydrogen Microgrid Model for Energy Management Applications

Marcos Tostado-Véliz[1], Paul Arévalo[1], and Francisco Jurado[1,*]

[1]*Department of Electrical Engineering, University of Jaén, 23700 EPS Linares, Jaén, Spain*

Abstract – Recently, a growing interest on multienergy Microgrids has been observed. This kind of grids involves different energy vectors and treat them on a whole. The most typical cases contemplate electrical, natural gas and hydrogen subsystems. Multiple efforts have been conducted on modelling this kind of grids for energy management problems. However, it is observed that most of references studied do not faithfully modelling this kind of grids or directly omit some of the mentioned subsystems, which difficults the accurately representation of these grids. This paper aims at developing a comprehensive but tractable yet multienergy MG model, which allows to accurately represent the interaction between electrical, natural gas and hydrogen subsystems. To that end, the developed framework includes detailed models of the different elements which are typically encountered in this kind of grids such as Gas-to-Power or Power-to-Gas facilities. Also, charging stations for electrical, natural gas and hydrogen vehicles are considered. Different tariffs and vehicle charging modes can be easily incorporated within the developed framework. The proposed model is validated with a case study in typical winter and summer scenarios based on real data. Results show that the developed model is able to accurately represent the operational behavior of multienergy Microgrids, which may be valuable for multiple research and educational tools.

Keywords: Multienergy Microgrid, Storage, Power to Gas

---

*Corresponding author, Tel.: +34 953 648518; Fax: +34 953 648586.

E-mail addresses: fjurado@ujaen.es (F. Jurado), mtostado@ujaen.es (M. Tostado), wpac0001@red.ujaen.es (P. Arévalo)

Nomenclature

Acronyms

MG Microgrid

RES Renewable Energy Source

ESS Electrical Storage System

EV Electric Vehicle

G2P Gas-to-Power

NG Natural Gas

NGV Natural Gas Vehicle

NGSS Natural Gas Storage System

P2G Power-to-Gas

P2H Power-to-Hydrogen (Electrolysis)

H2G Hydrogen-to-Gas (Methanation)

HSS Hydrogen Storage System

HV Hydrogen Vehicle

Variables

$P_t^{EG,buy}/P_t^{EG,sell}$ Power bought/sold from/to the electrical grid at time t [kW]

P_t^{RES} Power supplied by the RESs at time t [kW]

$\overline{P_t^{RES}}$ Capacity of RESs at time t [kW]

$P_t^{ESS,ch}/P_t^{ESS,dis}$ Power exchanged by the ESS with the MG in charging/discharging mode at time t [kW]

E_t^{ESS} Energy stored in the ESS at time t [kWh]

P_t^{G2P} Power supplied by the G2P unit at time t [kW]

P_t^{P2H} Input power of the P2G unit (Electrolysis process) at time t [kW]

$P_t^{Load,i}$ Electrical load at time t with tariff i [kW]

$P_t^{EVs,i}$ Power consumption of EVs at time t in charging mode i [kW]

$G_t^{NG,buy}/G_t^{NG,sell}$ NG bought/sold from/to the NG grid at time t [m³]

G_t^{G2P} Inflow of the G2P unit at time t [m³]

$G_t^{Co,in}/G_t^{Co,out}$ Inflow/Outflow of the NG compressor at time t [m³]

$G_t^{NGSS,in}/G_t^{NGSS,out}$ Inflow/Outflow of the NGSS at time t [m³]

G_t^{H2G} NG supplied by the P2G unit (Methanation process) at time t [m³]

$G_t^{NGVs,i}$ NG supplied to the NGVs at time t in charging mode i [m³]

$G_t^{Load,i}$ NG demand at time t with tariff i [m³]

H_t^{P2H} Hydrogen produced by the P2G (Electrolysis process) at time t [m³]

$H_t^{HSS,in}/H_t^{HSS,out}$ Inflow/Outflow of the HSS at time t [m³]

H_t^{H2G} Inflow of the P2G unit (Methanation process) at time t [m³]

$H_t^{HVs,i}$ Hydrogen supplied to the HVs at time t in charging mode i [m³]

I_t^i Commitment status of the dispatchable unit i at time t [Binary]

Parameters, Indexes & Constants

$\overline{P_{EG,buy}}/\overline{P_{EG,sell}}$ Electrical grid capacity to buy/sell electricity [kW]

$\overline{E_{ESS}}$ Capacity of the ESS [kWh]

G_i^{G2P}/P_i^{G2P} i^{th} point of the generation curve of the G2P unit for piecewise representation [m³/kW]

$\overline{P_{P2H}}/\underline{P_{P2H}}$ Maximum/Minimum capacity of the P2G unit (Electrolysis process) [kW]

$\overline{G_{NG,buy}}/\overline{G_{NG,sell}}$	NG grid capacity to buy/sell gas [m³]
$\overline{G_{Co}}$	Inflow/Outflow capacity of the NG compressor [m³]
$\overline{G_{NGSS,in}}/\overline{G_{NGSS,out}}$	Inflow/Outflow capacity of the NGSS [m³]
$\overline{G_{NGSS}}$	Capacity of the NGSS [m³]
$\overline{H_{HSS,in}}/\overline{H_{HSS,out}}$	Inflow/Outflow capacity of the HSS [m³]
$\overline{H_{HSS}}$	Capacity of the HSS [m³]
$\overline{H_{H2G}}/\underline{H_{H2G}}$	Maximum/Minimum capacity of the P2G unit (Methanation process) [m³]
RU_{EG}/RD_{EG}	Upward/Downward ramping limits of the electrical grid [kW]
RU_{G2P}/RD_{G2P}	Upward/Downward ramping limits of the G2P unit [m³]
RU_{NG}/RD_{NG}	Upward/Downward ramping limits of the NG grid [m³]
RU_{P2H}/RD_{P2H}	Upward/Downward ramping limits of the P2G unit (Electrolysis process) [kW]
RU_{H2G}/RD_{H2G}	Upward/Downward ramping limits of the P2G unit (Methanation process) [m³]
η_{tr}	MG coupling transformer efficiency [pu]
η_{RES}	RES efficiency [pu]
$\eta_{ESS,ch}/\eta_{ESS,dis}$	ESS efficiency in charging/discharging mode [pu]
η_{G2P}	G2P unit efficiency [pu]
η_{Co}	NG compressor efficiency [pu]
η_{Conv}	Converter efficiency [pu]
η_{P2H}	P2G unit efficiency (Electrolysis process) [pu]
DOD_{ESS}	Depth of discharge of the ESS [pu]
DOD_{NGSS}	Depth of discharge of the NGSS [pu]
DOD_{HSS}	Depth of discharge of the HSS [pu]

$E_{ESS,0}$	Initial charge of the ESS [kWh]
$G_{NGSS,0}$	Initial charge of the NGSS [m³]
$H_{HSS,0}$	Initial charge of the HSS [m³]
CF_{CH_4}	NG compressibility factor [pu]
CF_{H_2}	Hydrogen compressibility factor [pu]
$e2P$	Energy-to-power ratio [h]
$\Delta\tau$	Time step [h]
HHV_{H_2}	High heating value of the gaseous hydrogen [kWh/m³]
$\phi_{H_2 \to CH_4}$	$H_2 \to CH_4$ conversion factor [pu]
$\lambda_t^{EG,buy}/\lambda_t^{EG,sell}$	Cost of electrical energy bought/sold from/to the grid at time t [$/kWh]
λ_t^i	Price of electrical energy with tariff i or EV charging mode i at time t [$/kWh]
$\mu_t^{NG,buy}/\mu_t^{NG,sell}$	Cost of electrical NG bought/sold from/to the grid at time t [$/m³]
μ_t^i	Price of NG with tariff i or NGV charging mode i at time t [$/m³]
ν_t^i	Price of HV charging mode i at time t [$/m³]
i, j, k, m, n	Indexes of different tariffs or vehicle charging modes
T	Index of the last step of the evaluating period

1. Introduction

The increase in greenhouse gas emissions worldwide and the high price of fossil fuels, within an economy based on hydrocarbons, drive the development of new propulsion ecological technologies [1]. To reduce environmental pollution, MG concept must also adapt using clean alternatives such as RES that supply electric loads, natural gas or hydrogen loads [2]. In recent years there has been a growing interest in the so-called

multienergy MGs [3]. This kind of grids normally involve the interaction of different subsystems such as electrical, NG and hydrogen. The efficiency of a multi-energy system is greater than a system with a single source due to the complementarity of its resources, since electrical and NG systems can take advantage of renewable resources and low energy costs of the networks. The NG loads can be supplied through the electrical network or renewable sources and the electrical loads could be supplied through the NG network by using G2P and P2G units, so, the reliability is greater due to the high number of sources available [3–8]. Also, the consideration of different subsystems on a whole, is of value for MG operators, which may buy electricity or NG from the upscale grids and sell them to final consumers such as vehicles or residential buildings [9].

Currently, multi-energy MG with more than two different sources are being developed more frequently. A correct energy control that optimizes the operation of each energy source in real time and from the technical and economic point of view is investigated in [5,6,10,11], multiple sources make it possible to supply different types of loads at the same time, increasing the feasibility of system. A MG that supplies electrical and hydrogen loads simultaneously is studied in [12–17]. In the literature, the authors proposed stochastic optimization methods to design the MG powered by RES and a support diesel generator, the objective is to develop optimal operational strategies for maximize profits by selling electricity and hydrogen to the owners of HVs, the results show that the isolated MG are capable of meeting the demand of both types of vehicles at a low cost, minimizing the operation of the diesel generator [17]. Similarly, in [13] the authors perform the optimization of the MG that supplies EVs and HVs simultaneously based on robust non-stochastic programming, the results are encouraging from the technical and economic point of view. On the other hand, the same connected MG is analyzed with the aim of optimizing the energy exchange between sources and loads,

considering the availability of renewable resources and the cost of buying energy from the grid [14,15].

A multienergy MG to supply electric, NG and hydrogen loads has been analyzed so far only in [18]. The authors proposed a new approach to the management of energy for MG with electric vehicle chargers, hydrogen pumps and gas pumps. Forecasting methodologies for renewables, electricity price and traffic flow are also presented to support the modeling and operation of the MG. The results show that MG is viable and that an energy storage system can save up to $ 127 per day. However, the model studied in [18] does not present a complete energy exchange such as P2G or G2P units. In such a way that the viability increases using electricity or natural gas grid when necessary, that is, when grid costs are high, the MG will use electricity from RES or the ESS to supply demand, and when the price of the energy or gas is minimal, it will be used to buy and store energy, being able to freely exchange energy between the three systems. Furthermore, an economic study that benefits the MG owner considering the three technologies mentioned above and detailing opportunities to formulate more sophisticated business models based on the benchmark has not yet been conducted [9].

Inside the multienergy MG, NGVs are an alternative highly mentioned in the literature. By 2024 there will be around 30 million NGV vehicles worldwide [19], in some countries such as China [20] or Nigeria [21] report a great current and future development of NG grid with barriers to overcome, especially political ones. The first countries to use compressed NG were those with resources in their subsoil [22] today many countries use NG from the urban network. To be used the NG from the pipeline in the NGV, it is necessary to adapt it by means of certain equipment that is investigated in [22], an important component to optimize is the compressor [3], as well as the pressure and tank temperature [23,24]. The interaction between the NG network and the electrical grid or

RES requires an energy management strategy to minimize the operating costs [7]. In a multienergy system, the operation of a NG subsystem with electrical and NG loads considering uncertainties of RES such as wind turbines and photovoltaic pannels is analyzed in [7]. In [25], the authors apply the Monte Carlo simulation to solve the random behavior of RES in a system composed of NG and electricity, showing that the combination of the two technologies (electricity and heat) improves efficiency and reduces costs [26–30]. In this regards, there are many studies that analyze the optimization and energy management of a system composed of NG and electrical grid considering P2G energy exchange, and using different computational techniques from the economic and technical ones [8,31–35]. In [3], the authors analyze a multienergy MG to supply EVs and NGVs, based on RES (solar and wind), a P2G unit and a NG distributed generator. The proposed optimization is modeled as mixed integer linear programming. The results show that the economic benefits of the proposed MG are significantly greater than those of a conventional one.

This work aims at filling the gaps encountered on the multienergy MGs proposed so far, by proposing a novel comprehensive multienergy MG model suitable for energy management applications. The new proposal encompasses electrical, gas and hydrogen subsystems. The main idea behind the developed model is to find a compromise between completeness, accuracy and simplicity. As just examples of the gaps that our proposal aims at filling, let us summarize them in the following points. 1) Most works done so far are mainly focused on only one energy vector while the others are customary simplified. This is a good approach when a subsystem has to be further analyzed, however, it lacks of accurateness when the interactions occurred in the overall system shall to be observed. One clear example is the G2P unit, which is often modelled as a linear relationship between the inflow NG and the output power. However, as modelled this work, this

relationship is rather nonlinear. 2) To the best of our knowledge, any reference has studied the EV, NGV and HV refueling processes on a whole, which serves for exploring the interaction between these processes and the remainder grid. 3) Many works neglect the intermediate usages of hydrogen and even its storage system within the P2G paradigm, therefore, some hydrogen endings like HV refueling cannot be considered by using simpler models. Our proposal aims at filling these gaps. On the basis of these contributions, we find our proposal valuable for many research and educational purposes as it is preserved simple but accurate and detailed enough. The developed model is validated by carrying out an energy management problem in two typical winter and summer scenarios based on real data.

The remainder of this paper is organized as follows: Section 2 reviews the main elements involved in a multienergy MG. The mathematical modelling of the developed multienergy MG is introduced in Section 3. Section 4 presents a case study to prove the good performance of the developed model. Finally, the main conclusions are duly drawn in Section 5.

2. Description of Multienergy MGs

Multienergy MGs typically include a series of devices and elements which interact among them to supply and consume electricity, NG or hydrogen. The following points provide a brief description about the different elements that may have been encountered in this kind of MGs.

- *RESs*

Typically, a MG can obtain electrical energy from own resources such as wind turbines or photovoltaic panels. These resources are based on renewable energies and are subjected to the stochastic character of different natural resources like solar irradiance or wind

speed. The energy obtained from RESs is normally conditioned to the MG requirements by using electronic devices such as inverters.

- *Storage Systems*

Storage systems bring multiple advantages to MG operation. For example, they compensate the intermittent production of RESs or allow to storage resources in periods of low price to be consumed in peak periods. In multienergy MGs one may find ESSs, which store electrical energy. This process is normally carried out by using electrochemical process through batteries of different technologies. On the other hand, NG and hydrogen may be stored in gaseous stage. To be stored, both NG and hydrogen are normally previously compressed up to 200 bar and 700 bar, respectively.

- *G2P*

Multienergy MGs typically includes a G2P unit, which can convert a natural gas flux to electrical energy. Examples of G2P units are gas-fired turbines or gasifiers [36]. This kind of elements are attractive when the price of NG is sufficiently low to produce a profit in supplying electricity.

- *P2G*

The P2G is known as the set of activities conducted to convert electrical energy to NG. Different technologies are available to such end like alkaline electrolysis, polymer electrolyte membranes and solid oxide electrolysis [37]. In this work, a P2G model composed by three steps as showed in Fig. 1 has been considered. In a first step, the input electric power is used to produce hydrogen in a process called Electrolysis (P2H) [37]. During the Electrolysis, the P2G unit consumes electricity and water to produce hydrogen and oxygen. After that, the produced hydrogen is normally compressed up to 700 bar and stored. This hydrogen may be directly blended with NG in the local grid, however, many countries impose limitations in the amount of hydrogen that can be supplied [38]. So, in

this article is considered that the produced hydrogen is either supplied to HVs or to the Methanation process (H2G), which produces synthetic natural gas, heat, and water; while it consumes hydrogen and CO_2 [37].

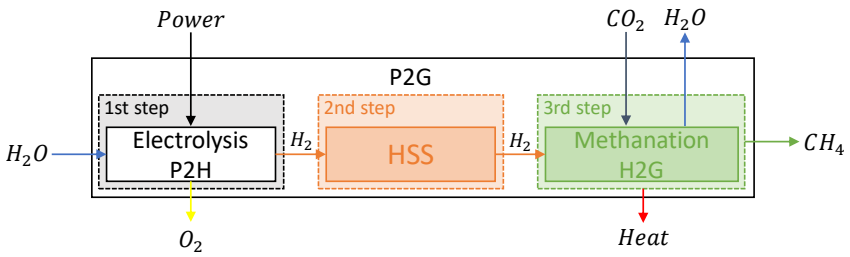

Figure 1. P2G process

- *Gas Compressors*

These devices are deployed through the MG to compress both NG and hydrogen to be stored. In both cases, they have to be considered as electrical loads.

3. Multienergy Microgrid Modelling

The modelling MG includes electrical, NG and hydrogen subsystems with different generators and loads. It also includes vehicle and local demands. Different components like compressors and storage systems are also modelled. In summary, Fig. 2 shows a schematic representation of the MG under study. The nomenclature used for modelling this MG is showed in its schematic representation of Fig. 2.

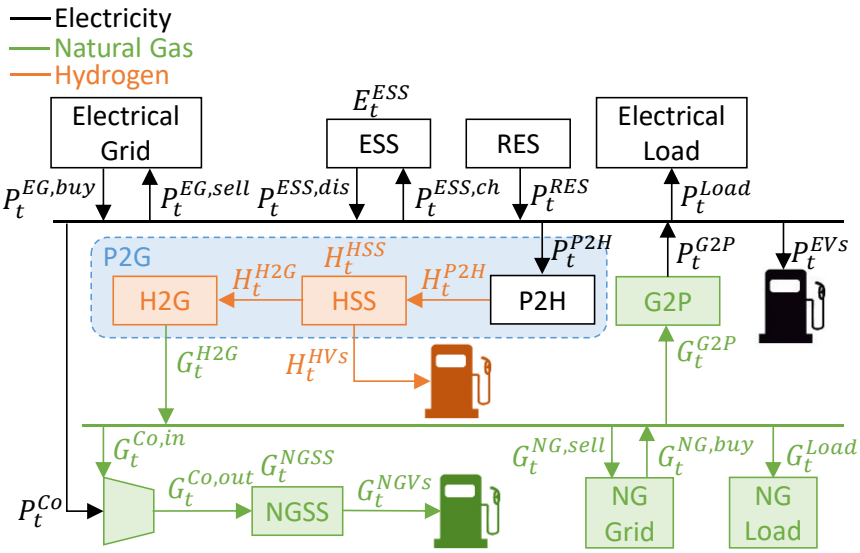

Figure 2. Schematic representation of the MG under study

- *Electrical Grid*

The modelled MG can buy or sell energy from/to an upscale grid. The amount of energy that can be bought/sold per unit of time is upper bounded in both cases by the equations (1) and (2). In addition, it is not possible to buy and sell electricity at the same period, as modelled the equation (3). The available power from/to the grid is also subjected to physical ramps limits, as represented the equations (4) and (5), which aims at modelling the low capacity reaction that can be experienced by some conventional units deployed through the utility grid.

$$0 \leq P_t^{EG,buy} \leq I_t^{EG,buy} \overline{P_{EG,buy}}, \forall t \quad (1)$$

$$0 \leq P_t^{EG,sell} \leq I_t^{EG,sell} \overline{P_{EG,sell}}, \forall t \quad (2)$$

$$0 \leq I_t^{EG,buy} + I_t^{EG,sell} \leq 1, \forall t \quad (3)$$

$$P_{t-1}^{EG,buy} - RD_{EG} \leq P_t^{EG,buy} \leq P_{t-1}^{EG,buy} + RU_{EG}, \forall t > 1 \quad (4)$$

$$P_{t-1}^{EG,sell} - RD_{EG} \leq P_t^{EG,sell} \leq P_{t-1}^{EG,sell} + RU_{EG}, \forall t > 1 \quad (5)$$

- *RES*

In this work, the different RES generators deployed such as photovoltaic panels or wind turbines are modelled as a unique generic generator. Typically, RES production is given in terms of availability of some natural resource such as solar irradiation or wind speed. In this paper, it is supposed that this data has been previously converted in terms of active power by using the component models available in multiple references (e.g. see [39]). The supplied power is upper bounded by the equation (6). The maximum delivered RES power is given by either physical component limits or the availability of the natural resource; so that, the upper limit in the equation (6) is a time-dependent variable rather than a constant.

$$0 \leq P_t^{RES} \leq I_t^{RES}\overline{P_t^{RES}}, \forall t \tag{6}$$

- *ESS*

The modelled MG encompasses an ESS, which is represented as a single system and can include different battery technologies for convenience. The ESS can absorb or deliver power from/to the MG, however, this value is limited bounded by the equations (7) and (8). In addition, the ESS cannot be charged and discharged at the same time as modelled the equation (9). The equation (10) models the state of charge of the ESS, which is upper and lower bounded by its nominal capacity and depth of discharge value, respectively, as represented the equation (11). Finally, the equations (12) and (13) represent the initial and final state of charge of the ESS.

$$0 \leq P_t^{ESS,ch} \leq I_t^{ESS,ch}\frac{\overline{E_{ESS}}}{e2P}, \forall t \tag{7}$$

$$0 \leq P_t^{ESS,dis} \leq I_t^{ESS,dis}\frac{\overline{E_{ESS}}}{e2P}, \forall t \tag{8}$$

$$0 \leq I_t^{EG,ch} + I_t^{EG,dis} \leq 1, \forall t \tag{9}$$

$$E_t^{ESS} = E_{t-1}^{ESS} + \left(P_t^{ESS,ch}\eta_{ESS,ch} - P_t^{ESS,dis}/\eta_{ESS,dis}\right)\Delta\tau, \forall t > 1 \tag{10}$$

$$(1 - DOD_{\text{ESS}})\overline{E_{ESS}} \leq E_t^{ESS} \leq \overline{E_{ESS}}, \forall t \tag{11}$$

$$E_1^{ESS} = E_{ESS,0} \tag{12}$$

$$E_{t=T}^{ESS} = E_1^{ESS} \tag{13}$$

- Gas-to-Power (G2P) Facility

Some works model the G2P facilities as a linear relationship between the input natural gas and the output power. However, as indicated in [40], this relationship is nonlinear. In this paper, similarly to [40], the G2P unit is modelled as a piecewise representation of the nonlinear relationship between the input natural gas and the output power as described the Fig. 3 and the equations (14)-(18).

$$P_t^{G2P} = \sum_{i=1}^{N} \left[I_{t,i}^{G2P} (K_i G_t^{G2P} + M_i) \right], \forall t \tag{14}$$

$$K_i = \frac{P_{i+1}^{G2P} - P_i^{G2P}}{G_{t,i}^{G2P} - G_{t,i}^{G2P}} \tag{15}$$

$$M_i = P_i^{G2P} - G_i^{G2P} K_i \tag{16}$$

$$0 \leq \sum_{i=1}^{N} I_{t,i}^{G2P} \leq 1 \tag{17}$$

$$I_{t,i}^{G2P} G_i^{G2P} \leq G_t^{G2P} \leq I_{t,i}^{G2P} G_{i+1}^{G2P} \tag{18}$$

The equation (14) introduces N bilinear terms which can be converted to linear variables [41].

As observed, the nonlinear curve in Fig. 3 is linearized by N different points. Intuitively, the higher N implies the more accurate representation of the curve in Fig. 3, however, the system become more complex and harder to be solved. It is worth observing that the input of the G2P unit is automatically lower and upper bounded by the piecewise representation of its nonlinear relationship ($I_{t,1}^{G2P} G_1^{G2P} \leq G_t^{G2P} \leq I_{t,N}^{G2P} G_N^{G2P}$). The G2P unit is also constrained by ramp limits, as modelled the equation (19).

$$G_{t-1}^{G2P} - RD_{G2P} \leq G_t^{G2P} \leq G_{t-1}^{G2P} + RU_{G2P}, \forall t > 1 \tag{19}$$

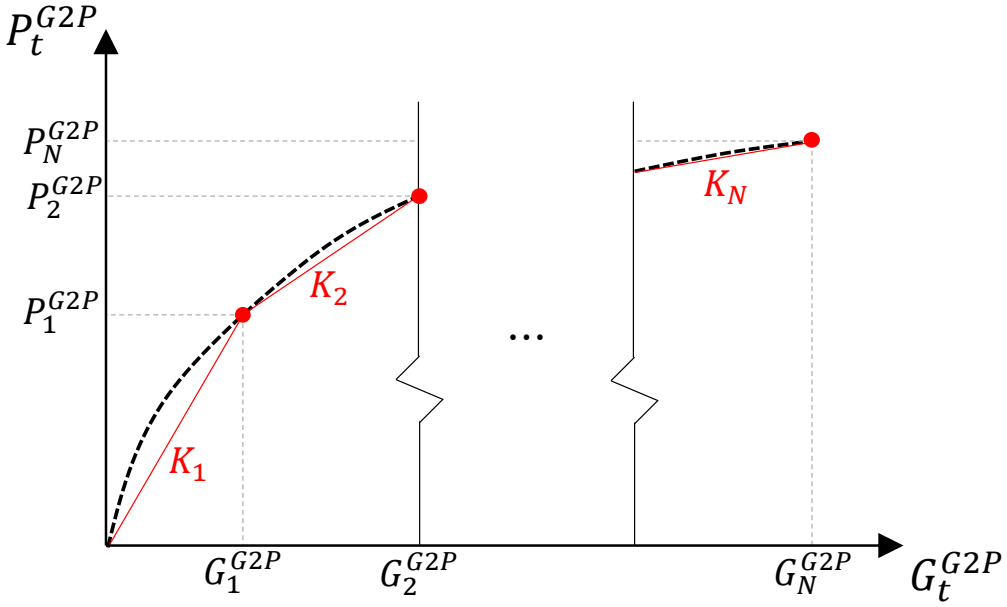

Figure 3. Piecewise representation of the G2P unit

- *NG Grid*

The natural gas grid is modelled similar to the electrical grid. Thus, a certain volume of natural gas may be bought or sold from/to the grid as indicated the equations (20) and (21). As the electrical grid, it is not possible buy and sell natural gas at the same time as modelled the equation (22). Finally, the equations (23) and (24) represent the ramp limits of this system.

$$0 \leq G_t^{NG,buy} \leq I_t^{NG,buy}\overline{G_{NG,buy}}, \forall t \quad (20)$$

$$0 \leq G_t^{NG,sell} \leq I_t^{NG,sell}\overline{G_{NG,sell}}, \forall t \quad (21)$$

$$0 \leq I_t^{NG,buy} + I_t^{NG,sell} \leq 1, \forall t \quad (22)$$

$$G_{t-1}^{NG,buy} - RD_{NG} \leq G_t^{NG,buy} \leq G_{t-1}^{NG,buy} + RU_{NG}, \forall t > 1 \quad (23)$$

$$G_{t-1}^{NG,sell} - RD_{NG} \leq G_t^{NG,sell} \leq G_{t-1}^{NG,sell} + RU_{NG}, \forall t > 1 \quad (24)$$

- *Gas Compressor*

Before supplying it to NGVs, the NG is compressed up to 200 bar and stored in gaseous stage [3]. The NG is compressed by using a multistage compressor, which consumes

active power and compresses a certain volume of NG. The equation (25) models the input-output relationship of the compressor.

$$G_t^{Co,out} = CF_{CH_4} G_t^{Co,in}, \forall t \quad (25)$$

It is worth noting that, although the power consumed by the gas compressor varies with its operating conditions, in this work a simplification by which this device is always supplied to its nominal power has been adopted. This has been done so because it has been observed that the gas compressors typically work to their nominal capacity, so, this simplification does not normally incur in large inaccuracies while it allows to preserve the model quite simple and computationally tractable.

Once the NG has been compressed up to the required pressure, it is stored into a NGSS; therefore, the output of the compressor is, in fact, the input of the NGSS as says the equation (26).

$$G_t^{NGSS,in} = G_t^{Co,out}, \forall t \quad (26)$$

The inflow/outflow NG to/from the compressor is subjected to limits as indicated the equations (27) and (28).

$$0 \leq G_t^{Co,in} \leq I_t^{Co} \overline{G_{Co}}, \forall t \quad (27)$$

$$0 \leq G_t^{Co,out} \leq I_t^{Co} \overline{G_{Co}}, \forall t \quad (28)$$

- *NGSS*

As mentioned, the compressed NG is stored before to be supplied to NGVs. The equation (29) models the output relationship of the NG stored and the compressed NG supplied to the NGVs. The volume of gas that can enter or leave the NGSS is bounded by the equations (30) and (31). As the ESS, the NGSS cannot absorb and supply NG at the same time as modelled the equation (32). The equation (33) represents the state of

charge of the NGSS. The total volume of NG stored is limited by the equation (34). Similarly, to the ESS, the equations (35) and (36) represent the initial and final state of charge of the NGSS, respectively.

$$G_t^{NGSS,out} = \sum_{\forall i} G_t^{NGVs,i}, \forall t \quad (29)$$

$$0 \leq G_t^{NGSS,in} \leq I_t^{NGSS,in}\overline{G_{NGSS,in}}, \forall t \quad (30)$$

$$0 \leq G_t^{NGSS,out} \leq I_t^{NGSS,out}\overline{G_{NGSS,out}}, \forall t \quad (31)$$

$$0 \leq I_t^{NGSS,in} + I_t^{NGSS,out} \leq 1, \forall t \quad (32)$$

$$G_t^{NGSS} = G_{t-1}^{NGSS} + G_t^{NGSS,in} - G_t^{NGSS,out}, \forall t > 1 \quad (33)$$

$$(1 - DOD_{NGSS})\overline{G_{NGSS}} \leq G_t^{NGSS} \leq \overline{G_{NGSS}}, \forall t \quad (34)$$

$$G_1^{NGSS} = G_{NGSS,0} \quad (35)$$

$$G_{t=T}^{NGSS} = G_1^{NGSS} \quad (36)$$

It is worth noting in equation (29) that different gas demand for NGVs have been considered. This has been done so to enable different fuelling modes. The reader can check that similar approaches have been adopted for EVs and HVs in other expressions.

- *Power-to-Gas (P2G) Facility*

As commented, the P2G facility encompasses three processes. In a first step, the Electrolysis process convert electrical power in hydrogen. The Electrolysis process is described by the equation (37). The required water may be acquired from a local grid while the input electricity is considered a variable and supplied by the MG. As observed, the produced hydrogen is also compressed to be posteriorly stored in gaseous stage [42]. In this paper, we consider that the power consumed by the associated compressor is included in the input power of the P2H unit (P_t^{P2H}).

$$H_t^{P2H} = \frac{P_t^{P2H} CF_{H_2} \eta_{P2H} \Delta\tau}{HHV_{H_2}} \quad (37)$$

The P2H unit is upper bounded as said the equation (38) and constrained by physical ramps as represented by the equation (39).

$$I_t^{P2H}\underline{P_{P2H}} \leq P_t^{P2H} \leq I_t^{P2H}\overline{P_{P2H}}, \forall t \quad (38)$$

$$P_{t-1}^{P2H} - RD_{P2H} \leq P_t^{P2H} \leq P_{t-1}^{P2H} + RU_{P2H}, \forall t > 1 \quad (39)$$

As mentioned, the produced hydrogen is compressed up to 700 bar and stored in an HSS. The HSS is modelled similarly to the NGSS by the equations (40)-(47).

$$H_t^{HSS,in} = H_t^{P2H}, \forall t \quad (40)$$

$$0 \leq H_t^{HSS,in} \leq I_t^{HSS,in}\overline{H_{HSS,in}}, \forall t \quad (41)$$

$$0 \leq H_t^{HSS,out} \leq I_t^{HSS,out}\overline{H_{HSS,out}}, \forall t \quad (42)$$

$$0 \leq I_t^{HSS,in} + I_t^{HSS,out} \leq 1, \forall t \quad (43)$$

$$H_t^{HSS} = H_{t-1}^{HSS} + H_t^{HSS,in} - H_t^{HSS,out}, \forall t > 1 \quad (44)$$

$$(1 - DOD_{HSS})\overline{H_{HSS}} \leq H_t^{HSS} \leq \overline{H_{HSS}}, \forall t \quad (45)$$

$$H_1^{HSS} = H_{HSS,0} \quad (46)$$

$$H_{t=T}^{HSS} = H_1^{HSS} \quad (47)$$

The produced hydrogen can be used to charge the HVs or as input to the third step of the P2G process called Methanation (H2G), as indicated the equation (48). The Methanation process is modelled by the Sabatier equation (49) and subjected to limits and ramps by the equations (50) and (51).

$$H_t^{HSS,out} = H_t^{H2G} + \sum_{\forall i} H_t^{HVs,i}, \forall t \quad (48)$$

$$G_t^{H2G} = H_t^{H2G}\phi_{H_2 \rightarrow CH_4}, \forall t \quad (49)$$

$$I_t^{H2G}\underline{H_{H2G}} \leq H_t^{H2G} \leq I_t^{H2G}\overline{H_{H2G}}, \forall t \quad (50)$$

$$H_{t-1}^{H2G} - RD_{H2G} \leq H_t^{H2G} \leq H_{t-1}^{H2G} + RU_{H2G}, \forall t > 1 \quad (51)$$

In this paper is assumed that the consumers do not demand heat, so that, although the produced heat may be used for multiple local endings, it is considered in this paper immaterial. On the other hand, the CO_2 system required to supply this element to the P2G chain has been neglected on the basis of two assumptions:

- The CO_2 required by the H2G process can be directly acquired from the atmosphere [42], therefore, it is not necessary an external source.
- The interactions between this system and the other main processes are considered immaterial as pointed out in [42].

- *Balance Equations*

Both the electrical and the NG system must satisfy the generation-load balance. In the case of the electrical system, the balance equation is given by

$$P_t^{EG,buy}\eta_{tr} + P_t^{RES}\eta_{RES} + P_t^{ESS,dis}/\eta_{ESS,dis} + P_t^{G2P}\eta_{G2P} = P_t^{EG,sell}/\eta_{tr} + P_t^{ESS,ch}\eta_{ESS,ch} + P_t^{P2H} + P_t^{Co}/\eta_{Co} + \frac{1}{\eta_{conv}}\sum_{\forall i} P_t^{EVs,i} + \sum_{\forall i} P_t^{Load,i}, \forall t \quad (52)$$

The different efficiencies are taken into account in this equation. It is considered that the MG is coupled with the transmission grid through a transformer with efficiency η_{tr}. It is assumed that the EVs charging is carried out through a AC/DC converter with efficiency η_{conv}. Similar devices are used for coupling the RESs with the MG, however, in this case it is assumed that the converter efficiency is considered with η_{RES}. Different electrical demands are considered in the equation (46) since various tariffs may be included. Similarly to (52), the equation (53) defines the generation-load balance of the NG system.

$$G_t^{NG,buy} + G_t^{H2G} = G_t^{NG,sell} + G_t^{G2P} + G_t^{Co,in} + \sum_{\forall i} G_t^{Load,i}, \forall t \quad (53)$$

Rightly, the hydrogen system should be also subjected to its own generation-load balance; however, this restriction has been already considered by the equations (40) and (48).

4. Case Study

- *Optimization Problem*

In order to validate the developed MG model, a 24h energy management optimization problem has been studied. The objective function for the case study will be the economic profit for the MG operator, as follows:

$$f = \sum_{\forall t} \Delta\tau \lambda_t^{EG,sell} P_t^{EG,sell} + \sum_{\forall i} \sum_{\forall t} \Delta\tau \lambda_t^i P_t^{Load,i} + \sum_{\forall j} \sum_{\forall t} \Delta\tau \lambda_t^j P_t^{EVs,j} +$$
$$\sum_{\forall t} \mu_t^{NG,sell} G_t^{NG,sell} + \sum_{\forall k} \sum_{\forall t} \mu_t^k G_t^{Load,k} + \sum_{\forall m} \sum_{\forall t} \mu_t^m G_t^{NGVs,m} +$$
$$\sum_{\forall n} \sum_{\forall t} \nu_t^m H_t^{HVs,n} - \sum_{\forall t} \Delta\tau \lambda_t^{EG,buy} P_t^{EG,buy} - \sum_{\forall t} \mu_t^{NG,buy} G_t^{NG,buy} \quad (54)$$

The first term in (54) are the revenues from selling electricity to the grid. The second and third terms are the revenues obtained from local electricity consumption and EV charging; both terms admit different tariffs and charging modes, respectively. Similarly, the fourth term in (54) are the revenues for selling NG, while the fifth and sixth terms are the revenues from local NG consumption and NGV charging, respectively. The hydrogen system brings revenues from charging HVs, as indicated the seventh term in (48). Finally, the last two terms of the objective function represent the cost from buying electrical energy and NG from the grid, respectively. Since the main purpose of this article is to validate the proposed multienergy MG model, maintenance and capital costs of the different components have been neglected in (54), in order to obtain results more easily interpretable. The case study consists of maximizing the economical profit as follows:

$$\max_{\boldsymbol{x}} f \quad (55a)$$

s.t.

$$\mathbf{g}(\boldsymbol{x}) \leq \mathbf{0} \tag{55b}$$

$$\mathbf{h}(\boldsymbol{x}) = \mathbf{0} \tag{55c}$$

In the problem (55), $\boldsymbol{x}$ is the vector of optimization variables while (55b) and (55c) are the set of inequalities and equalities constraints collected in equations (1)-(53), respectively. The problem (55) is a Mixed-Integer Linear problem which has been coded in Matlab R2019a, and solved with Gurobi [44]. In order to properly capture the different charging process and interactions, the problem has been solved with a time resolution of 5 minutes. Although faster processes occur in the MG (NG refuelling cycle), accumulated values can be taken to overcome this issue. On the other hand, different time scales restrictions have been already included by means of ramp constraints, which allows to take longer time steps. Nevertheless, the time step can be set as short as required, in order to further capture the different processes occurred in the MG, however, the computational effort employed in the resolution also grows.

- *Data*

The value of the different parameters involved in the problem (55) are collected in Table 1. Winter and summer scenarios are considered, Fig. 4 shows the electrical and NG demand for the studied scenarios, which are similar to those considered in [35,45]. While the electrical load is available with 5-min resolution, the NG demand is reported hourly; to adapt it to the time step using in this paper (5 min), it is supposed that the hourly gas demand is uniformly consumed.

Table 1 Value of the Parameters

Parameter	Value	Parameter	Value
$\overline{P_{EG,buy}}/\overline{P_{EG,sell}}$	2 MW/500 kW	η_{RES}	0.55
$\overline{E_{ESS}}$	750 kWh	$\eta_{ESS,dis}/\eta_{ESS,ch}$	0.95
$G_1^{G2P}, G_2^{G2P}, G_3^{G2P}, G_4^{G2P}$	0.1, 0.4, 0.7, 0.9 m³/min	η_{G2P}	0.95
$P_1^{G2P}, P_2^{G2P}, P_3^{G2P}, P_4^{G2P}$	50, 175, 230, 250 kW	η_{Co}	0.8
$\underline{P_{P2H}}/\overline{P_{P2H}}$	50/400 kW	η_{conv}	0.80
$\overline{G_{NG,buy}}/\overline{G_{NG,sell}}$	5/0.7 m³	η_{P2H}	0.77
$\overline{G_{Co}}$	3 m³	DOD_{ESS}	0.8
$\overline{G_{NGSS,in}}/\overline{G_{NGSS,out}}$	150 kg	DOD_{NGSS}	0.4
$\overline{G_{NGSS}}$	750 kg	DOD_{HSS}	0.4
$\overline{H_{HSS,in}}/\overline{H_{HSS,out}}$	3 m³	CF_{CH_4}	0.93
$\overline{H_{HSS}}$	6000 kg	CF_{H_2}	1.45
$\underline{H_{H2G}}/\overline{H_{H2G}}$	0.5/3 m³	$e2P$	4 h
RU_{EG}/RD_{EG}	500 kW	$\Delta\tau$	1/12 h
RU_{G2P}/RD_{G2P}	0.5 m³	HHV_{H_2}	39.8 kWh/m³
RU_{NG}/RD_{NG}	2 m³	$\phi_{H_2\to CH_4}$	4
RU_{P2H}/RD_{P2H}	100 kW	$E_{ESS,0}$	750 kWh
RU_{H2G}/RD_{H2G}	1 m³	$G_{NGSS,0}$	750 kg
η_{tr}	0.95	$H_{HSS,0}$	6000 kg

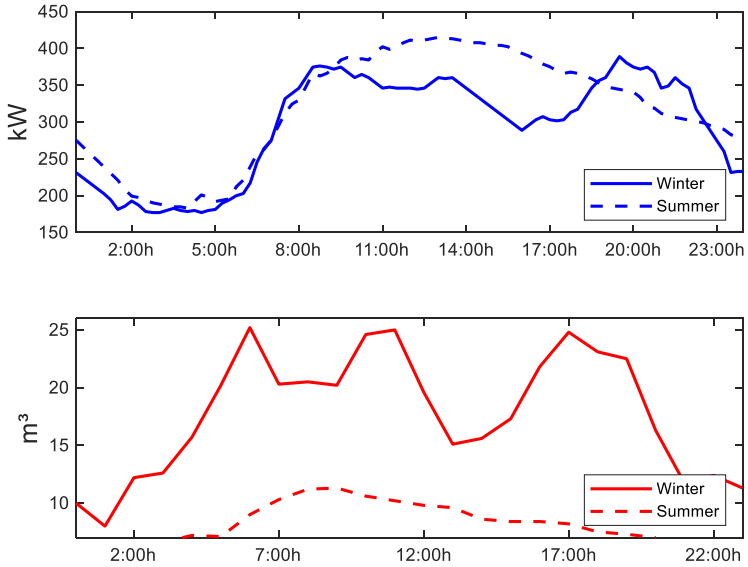

Figure 4. Electricity (upper) and NG (bottom) local demands

The EV, NGV and HV demand profiles have been built according to the vehicle trip distribution showed in [43] and are plotted in Fig. 5. These profiles have been built considering the characteristics of the different fuelling/charging modes and stations, which are reported in Table 2. In this paper, it has been assumed that the charging stations are only adapted for small vehicles, while larger ones like trucks could not be charged in the MG under study. The different charging costs have been taken similarly to those offered in Spain. In the case of EVs, the electrical demand during the charging process is not constant as showed in Fig. 6. In this case, a piecewise representation of the EV charging profiles has been considered. It is worth mentioning that the same vehicle demands have been used for the winter and summer scenarios.

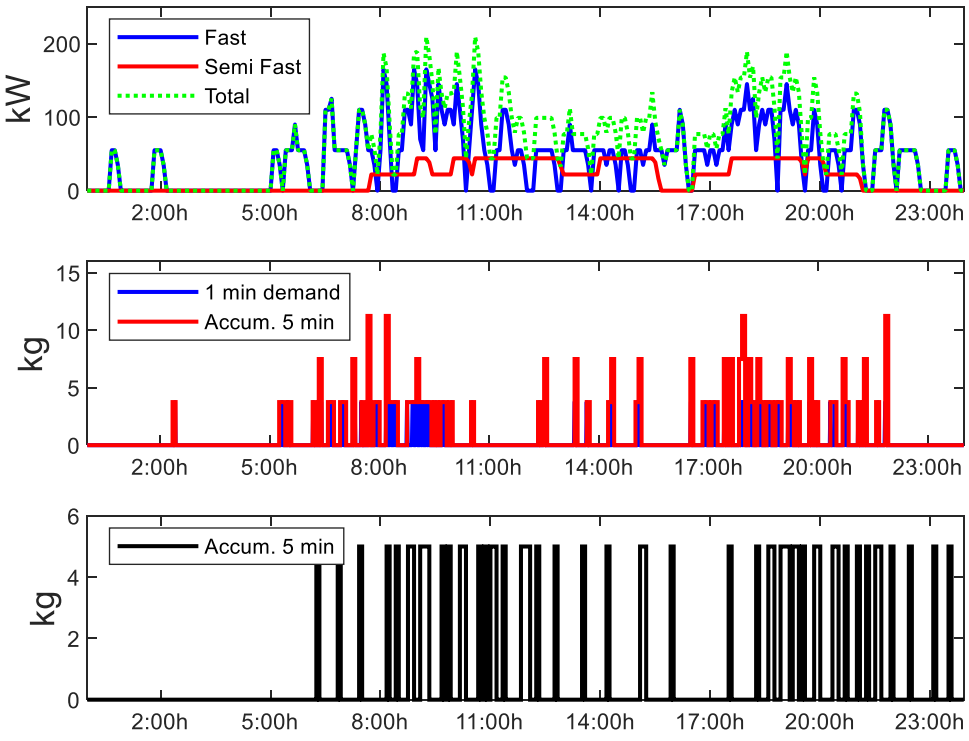

Figure 5. Demand of different vehicles. EVs (upper), NGVs (middle) and HVs (bottom)

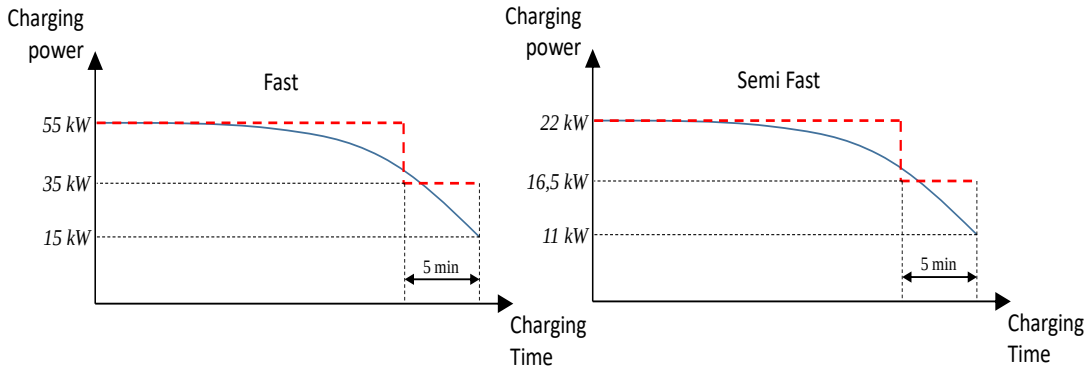

Figure 6. Demand profiles of the different EV charging modes and their piecewise representations used in simulations

Table 2 Characteristics of the Different Charging Modes for EVs, NGVs & HVs

Fuelling/Charging mode	Dispensers	Rating/Minimum power & rating flow	Fuelling/Charging time	Price
EV-Fast	3	55/15 kW	15-30 min	0.5 $/kWh
EV-Semi Fast	2	22/11 kW	1.5-3 h	0.2 $/kWh
NGV	1	4.3 kg/min	1-3 min	0.89 $/kg
HV	1	1 kg/min	5 min	7 $/kg

Table 3 shows the characteristics of the different electricity and NG tariffs considered for residential, industrial and commercial users. Three different electrical tariffs have been included which are like those offered by some companies in Spain. Typically, the consumers subjected to each tariff consume at those hours with low price. Under this assumption, a percentage of the electrical load will correspond to each tariff as showed Fig. 7. The hourly electricity and NG prices are showed in Fig. 8 [45]. The selling and buying prices are assumed to be the same. Photovoltaic and wind-based RESs are considered in this paper. The RES generation curves are showed in Fig. 9. They have been generated following the same patterns showed by the islanded grid of La Palma island (Spain), at typical winter and summer days [46].

Table 3 The Different Tariffs for Electricity & NG

Tariff	Price - Winter	Price - Summer
Electric 1	Fixed 0.15 $/kWh	Fixed 0.15 $/kWh
Electric 2	Variable 0.09 $/kWh 22-12h 0.18 $/kWh 13-21h	Variable 0.09 $/kWh 23-13h 0.18 $/kWh 14-22h
Electric 3	Variable 0.09 $/kWh 1-9h 0.15 $/kWh 7-12h	Variable 0.09 $/kWh 1-9h 0.15 $/kWh 7-12h
NG	Fixed 0.82 $/m³	Fixed 0.82 $/m³

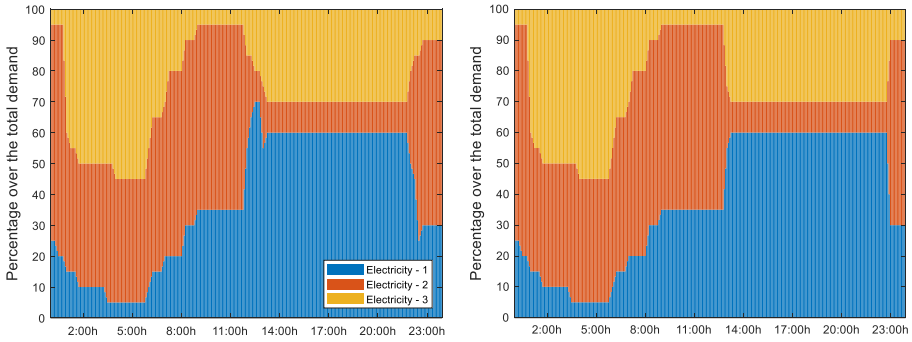

Figure 7. Percentage of the total electrical demand corresponding to consumers subjected to each electricity tariff at winter (left) and summer (right)

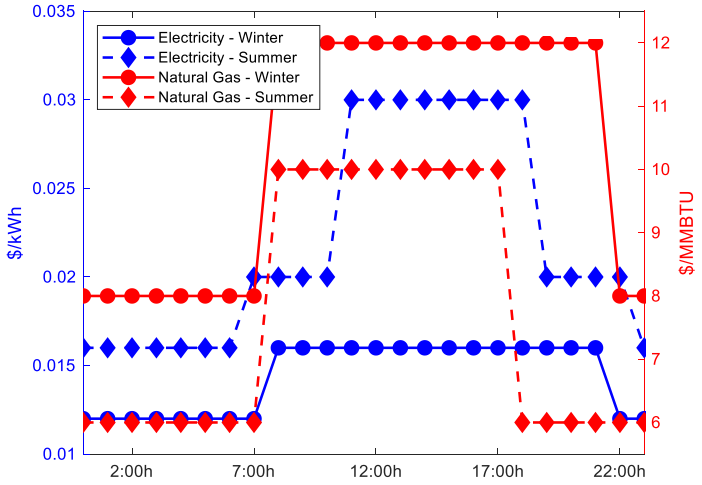

Figure 8. Electricity and NG buying prices

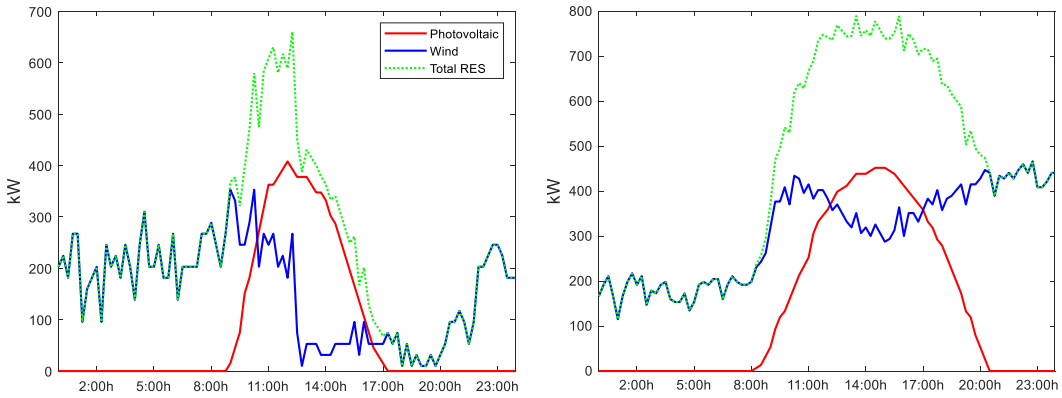

Figure 9. RES generation at winter (left) and summer (right)

It is worth mentioning that the different data has been considered here deterministic, which may be difficult to assert in the case of RES generation or the different demand profiles. However, the aim of this Section is just to demonstrate that the developed multienergy MG model works well and, consequently, it is not necessary to include any extra process to manage with the uncertainties brought by the different stochastic processes. Nevertheless, they can be treated using the proposed framework in the same manner as it is done in other works, for example, by using representative days [47].

- *Results. Winter scenario.*

The objective function (54) resulted in a profit of ~3888 $ for the winter scenario. Fig. 10 shows the RES and G2P production along the electricity bought and sold from/to the grid at winter scenario. As observed, the G2P production is kept almost constant during the whole day working at 31% of its nominal capacity. The MG under study demands much electricity from the grid (7.3 MWh), and it is only possible to sell ~5 kWh during the first hours of the day, promoted by a low electricity demand.

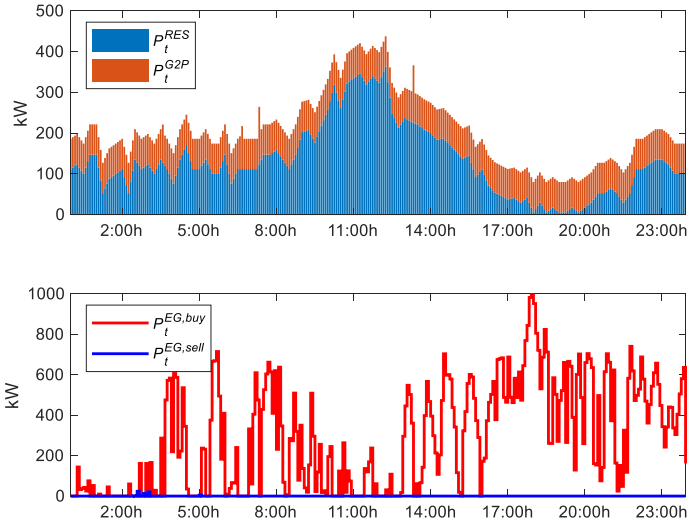

Figure 10. RES and G2P electricity generation (upper). Electricity bought and sold from/to the grid (bottom) at winter scenario

On the other hand, Fig. 11 plots the volumetric NG bought and sold from/to the NG grid along the NG produced by the H2G unit (methanation) at winter scenario. As observed, the H2G process allows to sell a considerable amount of NG to the grid (~65 m^3), which results in a considerable profit for the MG due to the high price of NG. In winter, the MG demands 318 m^3 of NG from the grid in a day. It is also worth noting that the MG sells electrical energy to the grid when the NG demand is fully supplied by the P2G unit. It indicates that it is more attractive to produce NG and selling it to the grid rather than generating a surplus electricity to sell it to the electrical grid. This behaviour is logic since the NG price is always much higher than the electricity price. Finally, Fig. 12 shows the performance of the different storage systems at winter scenario. As shown, the state of charge of the different storage systems is kept within limits.

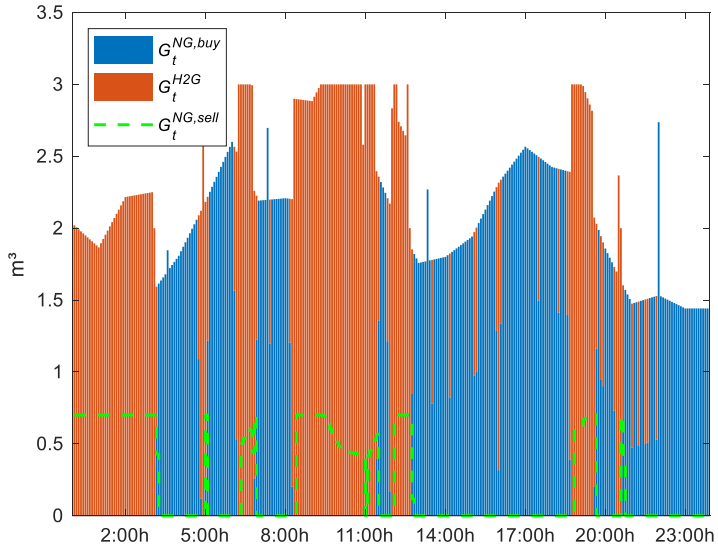

Figure 11. H2G production and NG bought/sold from/to the NG grid at winter scenario

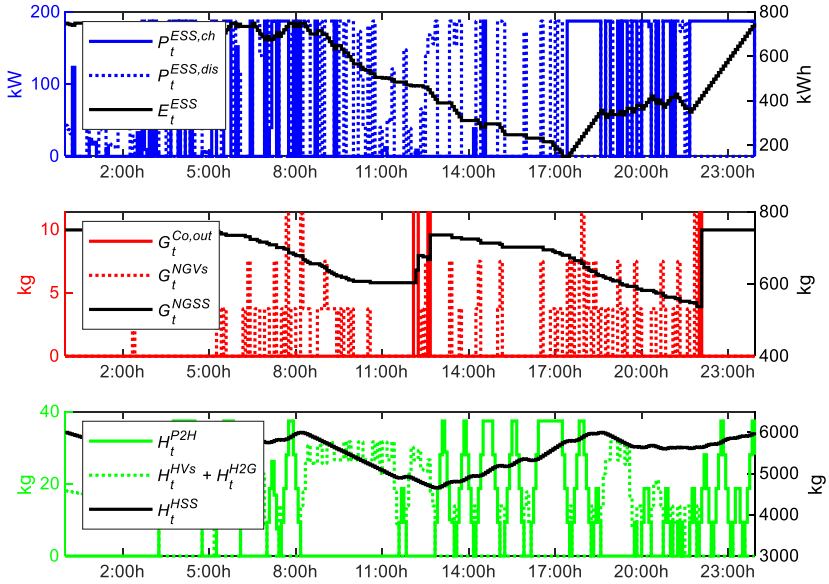

Figure 12. Performance of the different storage systems at winter scenario. ESS (upper), NGSS (middle) and HSS (bottom)

- *Results. Summer scenario.*

After carrying out the optimization problem (55), the objective function for the summer scenario yielded a profit of ~3861 $ at summer scenario. Fig. 13 plots the RES and G2P production along the electricity bought and sold from/to the grid at summer scenario. The G2P unit is more exploited in summer, achieving a production up to 175

kW. In this case, it is possible to sell up to 206 kWh to the grid. The energy bought from the grid was 3.6 MWh, much lower than at winter scenario, which is logic since the RES production is much higher in this case.

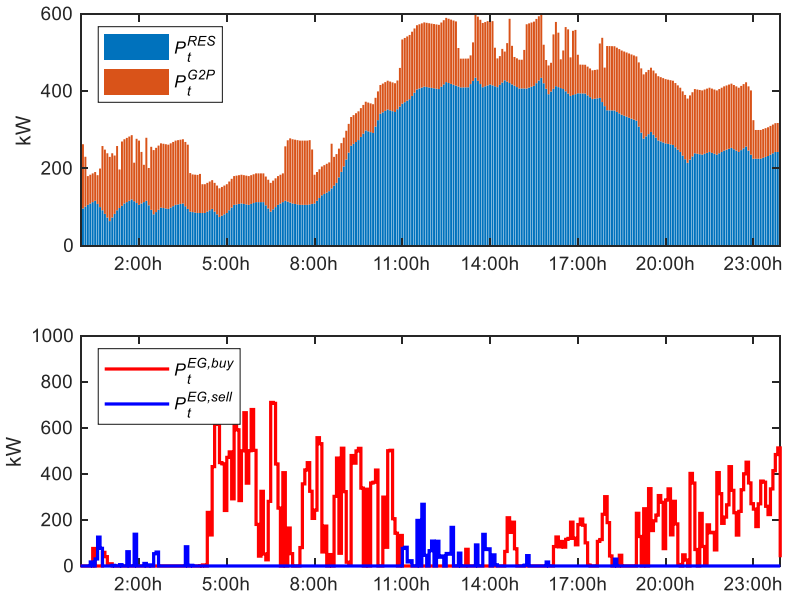

Figure 13. RES and G2P electricity generation (upper). Electricity bought and sold from/to the grid (bottom) at summer scenario

Figure 14 plots the volumetric NG bought and sold from/to the NG grid along the NG produced by the H2G unit at summer scenario. In this case, it is possible to sell up to 79 m^3 of NG to the grid, motivated by a low demand. This also benefits the G2P unit, which is more exploited than at winter scenario. In this scenario, the MG demands 236 m^3 of NG to the grid, much lower than in winter. Fig. 15 is analogue to Fig. 12 for the summer scenario, as observed, the developed MG model is able to accurately represent the behaviour of the different storage systems modelled.

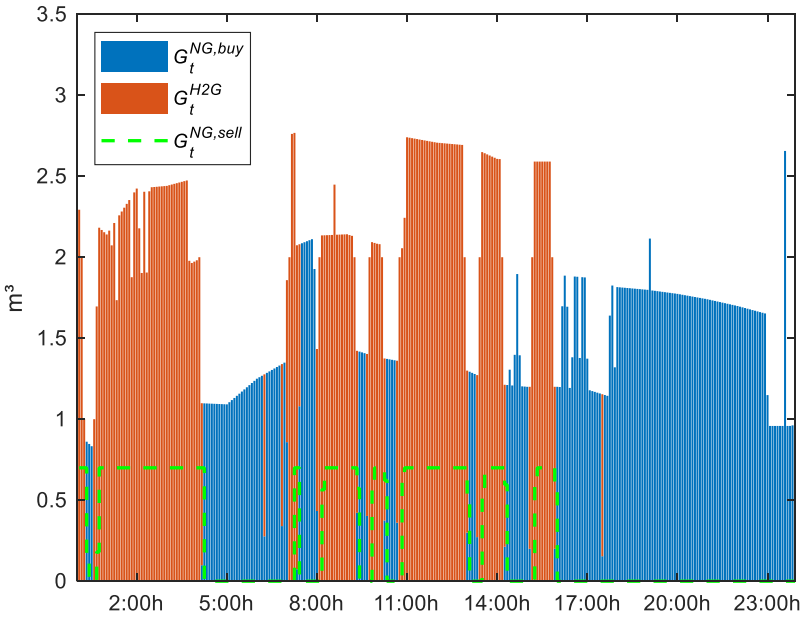

Figure 14. H2G production and NG bought/sold from/to the NG grid at summer scenario

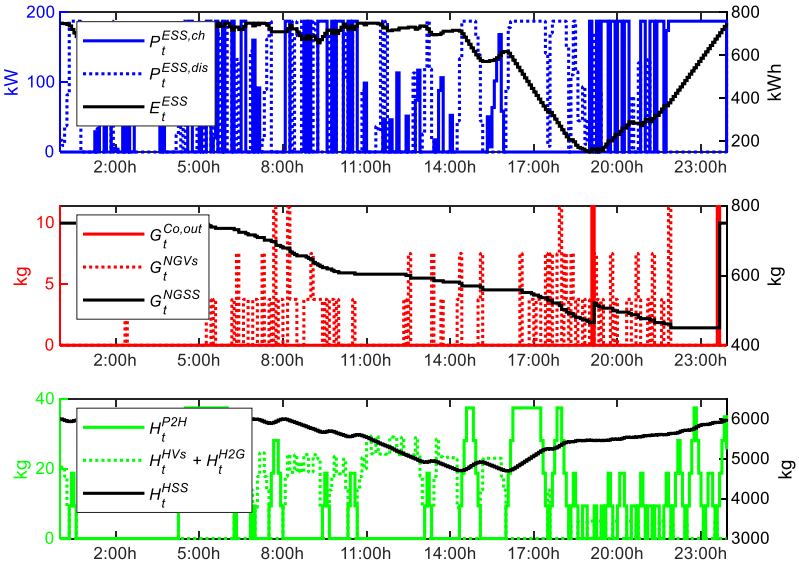

Figure 15. Performance of the different storage systems at summer scenario. ESS (upper), NGSS (middle) and HSS (bottom)

5. Conclusions

A comprehensive multienergy MG model has been presented. It aims at providing a simple but accurate enough model for electrical-gas-hydrogen MGs, in order to properly modelled the interactions among these systems without large computational requirements.

The proposal involves electrical, NG and hydrogen subsystems. Our framework is versatile enough to be adapted to any requirement as it includes the different elements that can be found in this kind of grids. Thus, the developed framework includes elements such as electrical and NG grids; RESs; comprehensive G2P and P2G models; different storage systems; vehicle demands; gas compressors; and local electrical and NG demands. In addition, our proposal also allows to include different electrical and NG tariffs along different charging modes for EVs; which makes it especially suitable for economic analysis. It is also worth mentioning that the developed model results in a mixed-integer linear problem which can be easily solved by using conventional software.

In order to validate our proposal, an energy management problem has been carried out in two typical winter and summer scenarios based on real data. The results have showed that the model coherently works. Thus, it is demonstrated the valuable contribution of our work in many areas related with energy management tools, as it allows to accurately simulate the interactions of the different systems involved while the model is preserved simple and tractable enough to be manage by average machines and tools.

Future works should be focused on further developing this kind of model to include security constraints and more detailed relationships with the main grids, in order to make it suitable for security applications.

References

[1] Hossain E, Kabalci E, Bayindir R, Perez R. Microgrid testbeds around the world: State of art. Energy Convers Manag 2014;86:132–53. https://doi.org/10.1016/j.enconman.2014.05.012.

[2] Ugirumurera J, Haas ZJ. Optimal Capacity Sizing for Completely Green Charging Systems for Electric Vehicles. IEEE Trans Transp Electrif 2017;3:565–77. https://doi.org/10.1109/TTE.2017.2713098.

[3] Faridpak B, Alahyari A, Farrokhifar M, Momeni H. Toward Small Scale Renewable Energy Hub-Based Hybrid Fuel Stations: Appraising Structure and Scheduling. IEEE Trans Transp Electrif 2020;6:267–77. https://doi.org/10.1109/TTE.2020.2972382.

[4] Battapothula G, Yammani C, Maheswarapu S. Multi-objective simultaneous optimal planning of electrical vehicle fast charging stations and DGs in distribution system. J Mod Power Syst Clean Energy 2019;7:923–34. https://doi.org/10.1007/s40565-018-0493-2.

[5] Akhtari MR, Baneshi M. Techno-economic assessment and optimization of a hybrid renewable co-supply of electricity, heat and hydrogen system to enhance performance by recovering excess electricity for a large energy consumer. Energy Convers Manag 2019;188:131–41. https://doi.org/10.1016/j.enconman.2019.03.067.

[6] Urbanucci L, Testi D, Bruno JC. An operational optimization method for a complex polygeneration plant based on real-time measurements. Energy Convers Manag 2018;170:50–61. https://doi.org/10.1016/j.enconman.2018.05.076.

[7] Kagiri C, Zhang L, Xia X. A hierarchical optimisation of a compressed natural gas station for energy and fuelling efficiency under a demand response program. Energies 2019;12. https://doi.org/10.3390/en12112165.

[8] Jiang Y, Xu J, Sun Y, Wei C, Wang J, Liao S, et al. Coordinated operation of gas-electricity integrated distribution system with multi-CCHP and distributed renewable energy sources. Appl Energy 2018;211:237–48. https://doi.org/10.1016/j.apenergy.2017.10.128.

[9] San Román TG, Momber I, Abbad MR, Sánchez Miralles Á. Regulatory framework and business models for charging plug-in electric vehicles: Infrastructure, agents, and commercial relationships. Energy Policy 2011;39:6360–75. https://doi.org/10.1016/j.enpol.2011.07.037.

[10] Jabari F, Mohammadi-ivatloo B, Bannae-Sharifian MB, Ghaebi H. Design and performance investigation of a biogas fueled combined cooling and power generation system. Energy Convers Manag 2018;169:371–82. https://doi.org/10.1016/j.enconman.2018.05.026.

[11] Gholamian E, Hanafizadeh P, Ahmadi P, Mazzarella L. A transient optimization and techno-economic assessment of a building integrated combined cooling, heating and power system in Tehran. Energy Convers Manag 2020;217:112962. https://doi.org/10.1016/j.enconman.2020.112962.

[12] Mehrjerdi H. Off-grid solar powered charging station for electric and hydrogen vehicles including fuel cell and hydrogen storage. Int J Hydrogen Energy 2019;44:11574–83. https://doi.org/10.1016/j.ijhydene.2019.03.158.

[13] Wang Y, Kazemi M, Nojavan S, Jermsittiparsert K. Robust design of off-grid solar-powered charging station for hydrogen and electric vehicles via robust optimization approach. Int J Hydrogen Energy 2020. https://doi.org/10.1016/j.ijhydene.2020.05.098.

[14] García-Triviño P, Torreglosa JP, Jurado F, Fernández Ramírez LM. Optimised operation of power sources of a PV/battery/hydrogen-powered hybrid charging station for electric and fuel cell vehicles. IET Renew Power Gener 2019;13:3022–32. https://doi.org/10.1049/iet-rpg.2019.0766.

[15] Sánchez-Sáinz H, García-Vázquez CA, Iborra FL, Fernández-Ramírez LM. Methodology for the optimal design of a hybrid charging station of electric and fuel cell vehicles supplied by renewable energies and an energy storage system.

Sustain 2019;11. https://doi.org/10.3390/su11205743.

[16] Mehrjerdi H, Bornapour M, Hemmati R, Ghiasi SMS. Unified energy management and load control in building equipped with wind-solar-battery incorporating electric and hydrogen vehicles under both connected to the grid and islanding modes. Energy 2019;168:919–30. https://doi.org/10.1016/j.energy.2018.11.131.

[17] Xu X, Hu W, Cao D, Huang Q, Liu W, Jacobson MZ, et al. Optimal operational strategy for an offgrid hybrid hydrogen/electricity refueling station powered by solar photovoltaics. J Power Sources 2020;451. https://doi.org/10.1016/j.jpowsour.2020.227810.

[18] Zhou S, Zhuang Y, Gu W, Wu Z. Operation and economic assessment of hybrid refueling station considering traffic flow information. Energies 2018;11. https://doi.org/10.3390/en11081991.

[19] NGV Statistics Updated | NGV Global Knowledgebase n.d. http://www.iangv.org/2016/12/ngv-statistics-updated/ (accessed August 17, 2020).

[20] Ma L, Geng J, Li W, Liu P, Li Z. The development of natural gas as an automotive fuel in China. Energy Policy 2013;62:531–9. https://doi.org/10.1016/j.enpol.2013.06.066.

[21] Ogunlowo OO, Bristow AL, Sohail M. Developing compressed natural gas as an automotive fuel in Nigeria: Lessons from international markets. Energy Policy 2015;76:7–17. https://doi.org/10.1016/j.enpol.2014.10.025.

[22] De Chauveron S. Natural gas for vehicles. Rev l'Institute Fr Du Pet 1996;51:729–41. https://doi.org/10.2516/ogst:1996048.

[23] Farzaneh-Gord M, Rahbari HR, Nikofard H. The effect of important parameters on the natural gas vehicles driving range. Polish J Chem Technol 2012;14:61–8. https://doi.org/10.2478/v10026-012-0104-3.

[24] Farzaneh-Gord M, Deymi-Dashtebayaz M. Optimizing natural gas fueling station reservoirs pressure based on ideal gas model. Polish J Chem Technol 2013;15:88–96. https://doi.org/10.2478/pjct-2013-0015.

[25] Qiao Z, Guo Q, Sun H, Pan Z, Liu Y, Xiong W. An interval gas flow analysis in natural gas and electricity coupled networks considering the uncertainty of wind power. Appl Energy 2017;201:343–53. https://doi.org/10.1016/j.apenergy.2016.12.020.

[26] Vazinram F, Hedayati M, Effatnejad R, Hajihosseini P. Self-healing model for gas-electricity distribution network with consideration of various types of generation units and demand response capability. Energy Convers Manag 2020;206:112487. https://doi.org/10.1016/j.enconman.2020.112487.

[27] Qaeini S, Nazar MS, Varasteh F, Shafie-khah M, Catalão JPS. Combined heat and power units and network expansion planning considering distributed energy resources and demand response programs. Energy Convers Manag 2020;211:112776. https://doi.org/10.1016/j.enconman.2020.112776.

[28] Alomoush MI. Microgrid combined power-heat economic-emission dispatch considering stochastic renewable energy resources, power purchase and emission tax. Energy Convers Manag 2019;200:112090.

https://doi.org/10.1016/j.enconman.2019.112090.

[29] Diaz C. JL, Ocampo-Martinez C, Panten N, Weber T, Abele E. Optimal operation of combined heat and power systems: An optimization-based control strategy. Energy Convers Manag 2019;199:111957. https://doi.org/10.1016/j.enconman.2019.111957.

[30] Olympios A V., Le Brun N, Acha S, Shah N, Markides CN. Stochastic real-time operation control of a combined heat and power (CHP) system under uncertainty. Energy Convers Manag 2020;216:112916. https://doi.org/10.1016/j.enconman.2020.112916.

[31] Liu C, Shahidehpour M, Wang J. Application of augmented Lagrangian relaxation to coordinated scheduling of interdependent hydrothermal power and natural gas systems. IET Gener Transm Distrib 2010;4:1314–25. https://doi.org/10.1049/iet-gtd.2010.0151.

[32] Du X, Yang X, Wang J, Wang G, Zhang Y. Coordinated optimal control strategy for multi-energy microgrids considering P2G technology and demand response. 2017 IEEE Conf. Energy Internet Energy Syst. Integr. EI2 2017 - Proc., vol. 2018- Janua, Institute of Electrical and Electronics Engineers Inc.; 2017, p. 1–6. https://doi.org/10.1109/EI2.2017.8245337.

[33] Li B, Roche R, Paire D, Miraoui A. Coordinated scheduling of a gas/electricity/heat supply network considering temporal-spatial electric vehicle demands. Electr Power Syst Res 2018;163:382–95. https://doi.org/10.1016/j.epsr.2018.07.014.

[34] Alabdulwahab A, Abusorrah A, Zhang X, Shahidehpour M. Coordination of Interdependent Natural Gas and Electricity Infrastructures for Firming the Variability of Wind Energy in Stochastic Day-Ahead Scheduling. IEEE Trans Sustain Energy 2015;6:606–15. https://doi.org/10.1109/TSTE.2015.2399855.

[35] Jiang Y, Guo L. Research on Wind Power Accommodation for an Electricity-Heat-Gas Integrated Microgrid System with Power-To-Gas. IEEE Access 2019;7:87118–26. https://doi.org/10.1109/ACCESS.2019.2924577.

[36] Vera D, Jurado F, Carpio J, Kamel S. Biomass gasification coupled to an EFGT-ORC combined system to maximize the electrical energy generation: A case applied to the olive oil industry. Energy 2018;144:41–53. https://doi.org/10.1016/j.energy.2017.11.152.

[37] Götz M, Lefebvre J, Mörs F, McDaniel Koch A, Graf F, Bajohr S, et al. Renewable Power-to-Gas: A technological and economic review. Renew Energy 2016;85:1371–90. https://doi.org/10.1016/j.renene.2015.07.066.

[38] Clegg S, Mancarella P. Integrated Modeling and Assessment of the Operational Impact of Power-to-Gas (P2G) on Electrical and Gas Transmission Networks. IEEE Trans Sustain Energy 2015;6:1234–44. https://doi.org/10.1109/TSTE.2015.2424885.

[39] Mandal S, Das BK, Hoque N. Optimum sizing of a stand-alone hybrid energy system for rural electrification in Bangladesh. J Clean Prod 2018;200:12–27. https://doi.org/10.1016/j.jclepro.2018.07.257.

[40] Wang S, Yuan S. Interval optimization for integrated electrical and natural-gas systems with power to gas considering uncertainties. Int J Electr Power Energy

Syst 2020;119:105906. https://doi.org/10.1016/j.ijepes.2020.105906.

[41] Khodaei A, Bahramirad S, Shahidehpour M. Microgrid Planning Under Uncertainty. IEEE Trans Power Syst 2015;30:2417–25. https://doi.org/10.1109/TPWRS.2014.2361094.

[42] He L, Lu Z, Zhang J, Geng L, Zhao H, Li X. Low-carbon economic dispatch for electricity and natural gas systems considering carbon capture systems and power-to-gas. Appl Energy 2018;224:357–70. https://doi.org/10.1016/j.apenergy.2018.04.119.

[43] Negarestani S, Fotuhi-Firuzabad M, Rastegar M, Rajabi-Ghahnavieh A. Optimal sizing of storage system in a fast charging station for plug-in hybrid electric vehicles. IEEE Trans Transp Electrif 2016;2:443–53. https://doi.org/10.1109/TTE.2016.2559165.

[44] Gurobi - The fastest solver - Gurobi n.d. https://www.gurobi.com/ (accessed September 3, 2020).

[45] Javadi MS, Lotfi M, Esmaeelnezhad A, Anvari-Moghaddam A, Guerrero JM, Catalao J. Optimal Operation of Energy Hubs Considering Uncertainties and Different Time Resolutions. IEEE Trans Ind Appl 2020:1–1. https://doi.org/10.1109/tia.2020.3000707.

[46] Inicio | Red Eléctrica de España n.d. https://www.ree.es/es (accessed September 3, 2020).

[47] García-Cerezo Á, Baringo L, García-Bertrand R. Representative Days for Expansion Decisions in Power Systems. Energies 2020;13:335. https://doi.org/10.3390/en13020335.